Phase unwrapping based on branch cut placing and reliability ordering

Yuangang Lu
Chinese Academy of Sciences
Shanghai Institute of Optics and Fine
 Mechanics
Information Optics Laboratory
P.O. Box 800-211
Shanghai 201800, China
 and
Graduate School of the Chinese Academy
 of Sciences
Beijing 100039, China
E-mail: lu_yuangang@siom.ac.cn

Xiangzhao Wang, MEMBER SPIE
Guotian He
Chinese Academy of Sciences
Shanghai Institute of Optics and Fine
 Mechanics
Information Optics Laboratory
P.O. Box 800-211
Shanghai 201800, China

Abstract. A new 2-D quality-guided phase-unwrapping algorithm, based on the placement of the branch cuts, is presented. Its framework consists of branch cut placing guided by an original quality map and reliability ordering performed on a final quality map. To improve the noise immunity of the new algorithm, a new quality map, which is used as the original quality map to guide the placement of the branch cuts, is proposed. After a complete description of the algorithm and the quality map, several wrapped images are used to examine the effectiveness of the algorithm. Computer simulation and experimental results make it clear that the proposed algorithm works effectively even when a wrapped phase map contains error sources, such as phase discontinuities, noise, and undersampling. © 2005 Society of Photo-Optical Instrumentation Engineers. [DOI: 10.1117/1.1911683]

1 Introduction

The ability to reconstruct a true phase field from the principal value of a wrapped phase is essential for many techniques that deal with coherent wave processes, such as optical interferometry, magnetic resonance imaging, and synthetic aperture radar interferometry.[1] In these techniques, the measured physical quantities are expressed in the form of a 2-D wrapped phase map. Since the wrapped phase map is defined by its principal values which range from $-\pi$ to π, phase unwrapping must be performed on the given phase map to obtain the original continuous phase field by removing the 2π phase jumps. Defects in the wrapped phase maps, such as phase discontinuities, noise, undersampling, and shadow, may produce unreliable phase data, which makes the recovery of a true phase map challenging.[2]

For more than 2 decades many phase-unwrapping algorithms have been proposed. These algorithms can be grouped into three classes:[3] (1) path-following algorithms, (2) region algorithms, and (3) global algorithms. Each of these algorithms is used to handle some sorts of problem successfully and each has its own drawbacks. The path-following algorithms are discussed briefly in the following because they are related to our new algorithm.

The path-following algorithms perform phase integration in a sequence of steps to recover the true phase field. They can be subclassified into three groups: (1) path-dependent algorithms, (2) residue-compensation algorithms, and (3) quality-guided algorithms.

The path-dependent algorithms[4] are the simplest among the path-following algorithms. They use an *a priori* defined search strategy, such as linear scanning, spiral scanning, and multiple direction scanning, to guide the phase integration process. Although these algorithms are usually fast, they are unable to handle noisy phase images because of the fixed data evaluation order.

The residue-compensation algorithms[5-8] search for residues in a wrapped phase image and place branch cuts between positive and negative residues. Because this procedure ensures that there is no rotational component in the phase field, path-independent unwrapped results can be obtained when the integration path does not cross the branch cuts. However, the unwrapping quality and the execution time of these algorithms depend on the branch cut generation criterion.

The quality-guided algorithms[9-12] use a quality map, which indicates the pixels' reliability of the wrapped phase map, to guide the integration path. They unwrap the highest quality pixels that have the highest reliability values first and the lowest quality pixels with the lowest reliability values last to prevent error propagation. Recently, Su and Chen[13] presented a review of these algorithms, and they demonstrated that their own quality-guided algorithm is effective on dealing with the complex fringe pattern. In general, the unwrapping quality of these algorithms depends on the quality map selection strategy. Because these algorithms do not generate branch cuts between residues, there is no guarantee that the integration path does not encircle an unbalanced residue and introduce a wrong 2π multiple error.

Some residue-compensation algorithms, such as Goldstein et al.'s algorithm,[5] may fail in the case that noisy phase data or undersampled data are present. This is due to the fact that the branch cuts are placed incorrectly. Part of the branch cuts misplaced in high-quality regions forces the integration path to cross low-quality regions that do not contain branch cut pixels. Thus, an unwrapped error occurs as these low-quality regions are crossed. To solve the prob-

lem, Flynn proposed a "mask cut algorithm,"[14] which uses a quality map to generate branch cuts in the wrapped maps. The algorithm starts at a residue and grows a pixel mask throughout the pixels of lowest quality. The growth stops when the total polarity of the residues in the mask is zero. This process is repeated until all residues in the mask are balanced. The mask is then thinned with morphological operators. Finally, the unwrapped result is obtained by simple path integration around the mask cuts. Because the branch cuts are reasonably confined to lie as much as possible within regions of low quality, the mask cut algorithm is successful in some applications,[15] such as interferometric synthetic aperture radar (IFSAR), magnetic resonance imaging (MRI), and simulated IFSAR. Despite its merits, the algorithm has its own disadvantages. In the path integration step, the algorithm discards the quality map and unwraps the wrapped phase by simple 1-D unwrapping along paths that avoid the mask. Because there is no guarantee that rather low quality pixels are all confined to the mask, the algorithm is certain to fail when the integration path first crosses these low-quality regions that are outside of the mask, especially when the wrapped phase map contains a high level of noise or complex discontinuities.

To overcome the drawbacks of the mask cut algorithm and produce a better phase-unwrapping path, this paper presents a new algorithm that combines the advantages of the residue-compensation algorithms and those of the quality-guided ones. The new algorithm falls into the quality-guided group. Its framework consists of branch cut placing guided by an original quality map and reliability ordering performed on a final quality map. First, a quality map, which can reflect the reliability of the wrapped phase image, is used as the original quality map to guide the placement of the branch cuts. This step balances all of the residues and confines the branch cuts to low-quality areas. Then the minimum quality value is assigned to branch cut pixels to generate a final quality map. Finally, the wrapped phase map is unwrapped based on the reliability ordering that is performed on the final quality map. The highest quality pixels with the highest reliability are integrated first and the pixels with gradually decreasing reliability are integrated in sequence. In this step, the algorithm searches the 8 neighboring pixels of the being processed pixel for the local minimum quality. Thus, it can be expected to generate a more reliable unwrapping path than that by means of searching for the 4 neighboring pixels of the pixel being processed.[13] The new algorithm automatically places branch cuts and unwraps the wrapped phase data without the necessity of thresholds and user interruption. Because the phase-unwrapping path does not encircle any unbalanced residue and is always along the way from a higher reliable area to the area with low reliability, even in the worst case, the phase-unwrapping error, if any, is limited to local minimum regions.

In the new algorithm, selecting a suitable quality map as the original quality map to guide the placement of the branch cuts is important. Although intensity modulation[16] is a useful quality map and was successfully used to generate branch cuts in the method for phase-stepping grating profilometry of complex objects, it must be calculated from original fringe patterns, which is not convenient and may not be available in many other applications related to phase
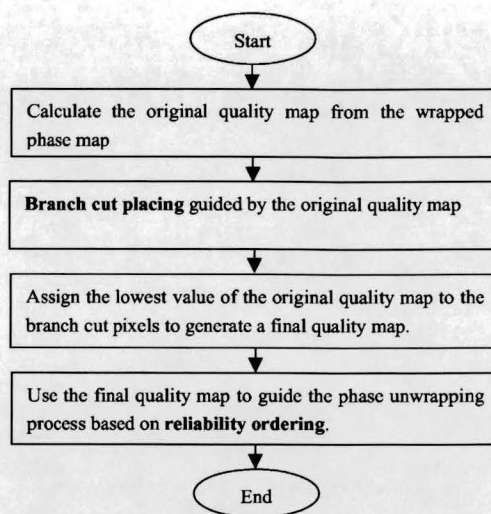

Fig. 1 Flow chart of the proposed algorithm.

unwrapping. Thus, we prefer to use other quality maps that can be directly derived from the wrapped phase data. In the proposed algorithm, any quality map directly derived from the wrapped phase data can be chosen as the original quality map. However, just as in any kind of quality-guided algorithm, the successful implementation of the algorithm largely relies on the accuracy of the quality map. Hence, we also propose a new quality map used as the original quality map to ensure a more reliable unwrapped result. Computer simulation and experiments verify the effectiveness of the new algorithm and the new quality map.

2 Principle

For better understanding, a simple flowchart for the proposed algorithm is illustrated in Fig. 1. The new algorithm uses an original quality map to generate the branch cuts, which are limited to lie as much as possible within low-quality areas. Then the position information of the branch cut pixels is used to generate a final quality map. Finally, the reliability ordering operation is performed on the final quality map, which determines an optimal phase-unwrapping path. In this section, we explain two critical steps of the proposed algorithm: branch cut placing guided by the original quality map and phase unwrapping based on reliability ordering.

2.1 Branch Cut Placing

Two-dimensional phase unwrapping is essentially a line integral process that can be represented by the following mathematical expression:

$$\varphi(x,y) = \int_C \left[\frac{\partial \phi(x,y)}{\partial x} dx + \frac{\partial \phi(x,y)}{\partial y} dy \right] + \varphi(x_0, y_0), \quad (1)$$

where C is any path within the wrapped phase map connecting the points (x_0, y_0) and (x,y), $\phi(x,y)$ is the wrapped phase value of the point (x,y), and $\varphi(x_0, y_0)$ and $\varphi(x,y)$ are the unwrapped phase values corresponding to points (x_0, y_0) and (x,y), respectively.
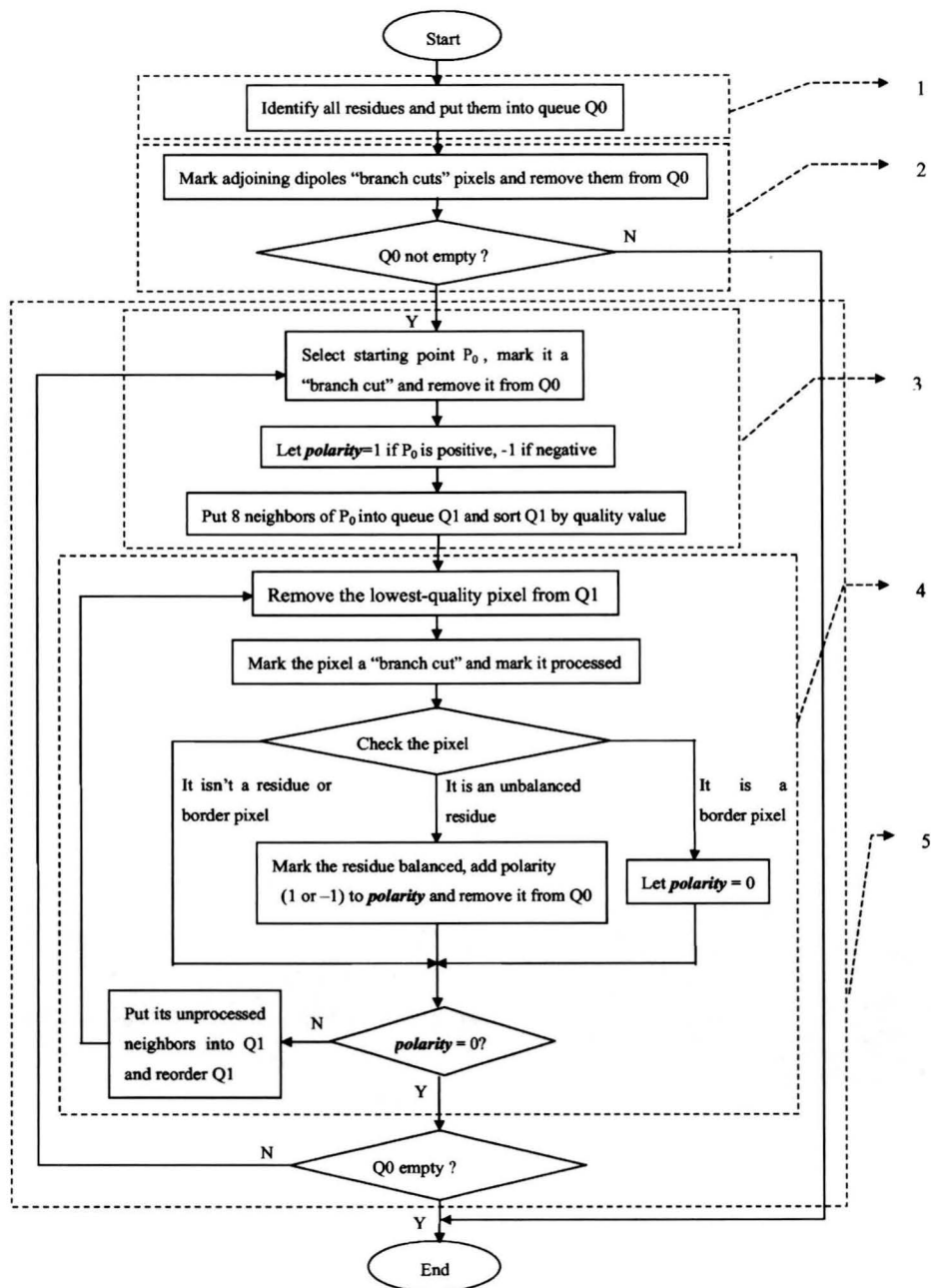
Fig. 2 Flow chart of the procedure of branch cut placing.

Theoretically, $\phi(x,y)$ is unique, in other words, phase unwrapping is path-independent, when the condition of the Shannon sampling theory is met. However, in practice, phase unwrapping is path-dependent for the reasons such as phase discontinuities, noise, and undersampling. In such situations, there are some phase residues in the wrapped phase map. If the integration path circles several phase residues, the closed-path integral result can be expressed as

$$\oint \left[\frac{\partial \phi(x,y)}{\partial x} dx + \frac{\partial \phi(x,y)}{\partial y} dy \right] = 2\pi \sum c_k , \qquad (2)$$

where the subscript k represents the order of a residue, and c_k is the corresponding polarity of the residue, which is 1 or -1. To obtain a path-independent unwrapped result, a residue polarity balance operation, branch cuts placing, is necessary to make the value of closed-path integral equal to 0. Since integration path will be around the branch cuts, the branch cuts are expected to lie as much as possible within low-quality areas, to limit the unavoidable unwrapping error, if any, within a local minimum area. Thus, a quality map can be used as a reasonable guide to grow the branch cuts. The quality map used to place branch cut is called the "original quality map." The original quality map can be

any one of those directly derived from the wrapped phase map, such as the variance of phase derivatives, maximum phase gradient or correlation coefficients.[15]

After the original quality map is directly obtained from the wrapped phase map, the procedure of branch cut placing is performed as follows (Fig. 2):

1. Identify each residue from the wrapped phase map and put all residues into an empty queue Q_0.

2. Mark each "adjoining dipole," two adjoining residues of opposite polarity, as branch cut pixels and remove them from Q_0. If Q_0 is empty, that is, all residues have been balanced, the branch cut placing is finished.

3. Take any residue in queue Q_0 as starting point, mark it a "branch cut" pixel and remove it from Q_0. Let a variable *polarity*$=1$ if P_0 is positive, or *polarity*$=-1$ if P_0 is negative. Then put 8 neighboring pixels of P_0 into an empty queue Q_1 and sort them by quality value.

4. Take out the lowest-quality pixel from queue Q_1. Mark the pixel a "branch cut" and mark it processed. There are three possible cases that the pixel belongs to. When the pixel is an unbalanced residue, mark the residue balanced, remove it from Q_0 and add its polarity (1 or -1) to *polarity*. When the pixel is a border pixel, let *polarity*$=0$. When the pixel is neither unbalanced residue nor border pixel, keep *polarity* unchanged. Then check the value of *polarity*. If *polarity*$\neq 0$, insert the unprocessed pixels of the pixel's 8 neighbors into Q_1 and reorder Q_1 by quality value. Repeat this step until *polarity*$=0$, that is, the branch cuts contain border pixel or equal number of opposite residues.

5. Repeat step 3 and 4, until queue Q_0 is empty. The procedure of branch cut placing is finished.

Because the branch cut pixels are unwrapped latest, these pixels can be considered as lowest reliability ones whose quality is the lowest. Thus, it is reasonable to replace the quality value of the branch cut pixels with the minimum value of the original quality map to generate a final quality map, which is used to produce an optimized phase unwrapping path based on reliability ordering.

2.2 Phase Unwrapping Based on Reliability Ordering

During the phase-unwrapping step, to ensure that low-reliability phase does not affect high-reliability phase, the reliability ordering must be performed so that the new algorithm unwraps the high-quality phase at an early stage and the low-quality phase at a later stage. Because a reliable original quality map is selected and an operation of branch cut placing is performed, the final quality map can be expected to truly reflect the reliability of the wrapped phase map. Therefore reliability ordering can be realized through quality ordering performed on the final quality map. Phase unwrapping based on reliability ordering is as follows:

1. Order all the quality value in the final quality map and take the highest quality pixel as the start point of phase unwrapping. Put its 8 neighboring pixels into a queue Q_2 and order them from higher quality to lower one.

2. Remove the highest quality pixel from Q_2 and unwrap the pixel on the basis of the start point. If the absolute difference between this pixel and the start point is less than π, the true phase of this pixel will equal its wrapped phase. If the difference between the two pixels is more than π, the true phase will equal its wrapped phase with 2π subtracted. If the difference is less than $-\pi$, the true phase equals its wrapped phase with 2π added. After this pixel has been unwrapped, mark this pixel as processed pixel, and insert the unprocessed pixels of its eight neighbors into Q_2 and reorder the queue by quality value.

3. Remove the highest quality pixel from Q_2 and unwrap the point on the basis of the immediately preceding unwrapped pixel. Mark this pixel as processed pixel, then insert the unprocessed pixels of its eight neighbors into Q_2 and reorder the queue by quality value.

4. Repeat steps 2 and 3 until the queue Q_2 is empty.

3 New Quality Map

As pointed out in Sec. 2, in the new algorithm, any existing quality map directly derived from the wrapped phase map can be chosen as the original quality map to guide the placement of the branch cuts. However, these existing quality maps have their own disadvantages. For example, correlation map is only available for SAR data. Phase derivative variance map, which is generally believed as the most reliable measure of phase quality,[15] cannot be responsive to highly varying regions that have been corrupted by undersampling when these regions may have good phase quality and therefore high-quality values. In this section, we present a new quality map that can overcome the drawbacks of the phase derivative variance map and thus ensure that unwrapped results are more reliable.

The proposed quality map is a hybrid from pseudocorrelation map[15] and phase derivative variance map. Regardless of the fact that pseudocorrelation map is not as effective as phase derivative variance map in many cases, it is sensitive to rapid changes and able to recognize the phase data with undersampling by assigning them with low-quality values. Therefore, the combination of the two quality maps can be expected to generate a better one.

The new quality map is defined by the equation

$$q_{m,n} = \frac{\left[\sum_{i=m-l/2}^{m+l/2}\sum_{j=n-l/2}^{n+l/2}(\Delta_{i,j}^x - \overline{\Delta_{m,n}^x})^2\right]^{1/2} + \left[\sum_{i=m-l/2}^{m+l/2}\sum_{j=n-l/2}^{n+l/2}(\Delta_{i,j}^y - \overline{\Delta_{m,n}^y})^2\right]^{1/2}}{l \times l}$$
$$\times \left\{ 1 - \frac{\left[(\sum_{i=m-l/2}^{m+l/2}\sum_{j=n-l/2}^{n+l/2}\cos\phi_{i,j})^2 + (\sum_{i=m-l/2}^{m+l/2}\sum_{j=n-l/2}^{n+l/2}\sin\phi_{i,j})^2\right]^{1/2}}{l \times l} \right\}, \tag{3}$$

where the quality of the pixel (m,n) is calculated from its $l \times l$ neighborhoods. The terms $\Delta_{i,j}^x$ and $\Delta_{i,j}^y$ are the partial derivatives of the phase. The term $\phi_{i,j}$ is the wrapped phase value. The terms $\Delta_{i,j}^x$ and $\Delta_{i,j}^y$ can be computed by the formulas

$$\Delta_{i,j}^x = W(\phi_{i+1,j} - \phi_{i,j}), \tag{4}$$

and

$$\Delta_{i,j}^y = W(\phi_{i,j+1} - \phi_{i,j}). \tag{5}$$

Note that $\overline{\Delta_{i,j}^x}$ and $\overline{\Delta_{i,j}^y}$ are the mean values of the partial derivatives of the phase in the $l \times l$ window. Also, W is the wrapping operator

$$W(\phi_{i,j}) = \phi_{i,j} + 2\pi k_{i,j}, \tag{6}$$

and $k_{i,j}$, an unknown integer, is chosen in such a way that $W(\phi_{i,j}) \in (-\pi, \pi)$.

From the preceding equations we know that the proposed quality map is directly derived from the wrapped phase map. The new quality map can truly reflect phase quality. In the areas where discontinuities, noise, and undersampling appear, the phase data are unreliable and should be recognized in the quality map. Discontinuities and noise in the unwrapped phase must be restricted to areas of noise and true discontinuity in the profile. Such areas can be successfully identified by their low quality in the proposed quality map. The quality map also can be effectively responsive to corrupted pixels that have been corrupted by undersampling caused by abrupt changes in the true profile. In this case, such pixels are assigned low-quality values, though these pixels may have good image quality. In Sec. 4, experimental results of the proposed quality map are compared with those obtained by use of the phase derivative variance map.

4 Simulated and Experimental Results

4.1 Simulated Results

The proposed algorithm was tested by use of two simulated images. In all wrapped phase images, wrapped phase is scaled so that black represents $-\pi$ rad and white represents π rad. Unwrapped phase images are also scaled between black and white to cover the full dynamic range.

Figure 3(a) shows a very noisy wrapped phase map of a simulated spherical surface. The wrapped phase map is 512 $\times$512 pixels in size and contains 19,908 residues. This image was used to test the proposed algorithm under noisy conditions. The root mean square (rms) deviation of Fig. 3(a) is 2.327 rad when it is compared with the correspond-

ing ideal wrapped spherical surface with no noise present. Figure 3(b) shows the unwrapped phase map obtained by using mask cut algorithm with the phase derivative variance map. There are some apparent unwrapped errors in the area of black speckles. The rms deviation of Fig. 3(b) is 4.588 rad when it is compared with the ideal unwrapped spherical surface. Figures 3(c) and 3(d) present the unwrapped results using the proposed algorithm with the phase derivative variance map and the new quality map, respectively. When the two unwrapped results are compared with the ideal unwrapped sphere surface, the rms deviations of Figs. 3(c) and 3(d) are 0.644 and 0.152 rad, respectively. The corresponding 3-D rendering of Figs. 3(b), 3(c), and 3(d) are shown in Figs. 3(e), 3(f), and 3(g), respectively.

Figure 4(a) shows a simulated wrapped phase image with surface discontinuities. The size of the image is 512 $\times$512 pixels. In this case, two planar surfaces were tilted relative to one another, creating a boundary of spiral sheared between them. Note that the presence of the phase discontinuities that must be taken into account in the unwrapping makes this image a difficult one to unwrap. The result unwrapped using the mask cut algorithm with the phase derivative variance map is shown in Fig. 4(b). The result shows the propagation of errors, originating at the physical profile discontinuity, throughout the entire image. The results unwrapped using the proposed algorithm with the phase derivative variance map and the new quality map are shown in Figs. 4(c) and 4(d), respectively. Both of these two unwrapped images are visually convincing that the unwrapping is qualitatively correct.

Although the two unwrapped results seem identical in appearance, there is a minute difference between them. Figure 4(e) shows the true phase value variation on a cross section of Fig. 4(c) when $x = 412$ pixels. There is a sudden, transient oscillation in the boundary of the sheared planar surfaces. Figure 4(f) shows the true phase value variation on the same cross section of Fig. 4(d). As we can see, the boundary is correctly upright and sharp.

The simulation results show that the proposed algorithm has a better ability to deal with noisy data and complex phase discontinuities. By using the new quality map as the original quality map to guide the placement of the branch cuts, the proposed algorithm can generate a more reliable unwrapped result.

4.2 Experimental Results

In our experiment the endface of a fiber optical connector was measured. The fiber undercut and the apex offset of the fiber connector are larger than those of an ordinary fiber connector. By using four-step phase-shifting interferometry, the wrapped phase map of a section of the fiber connector endface is obtained, which is shown in Fig. 5(a). The new
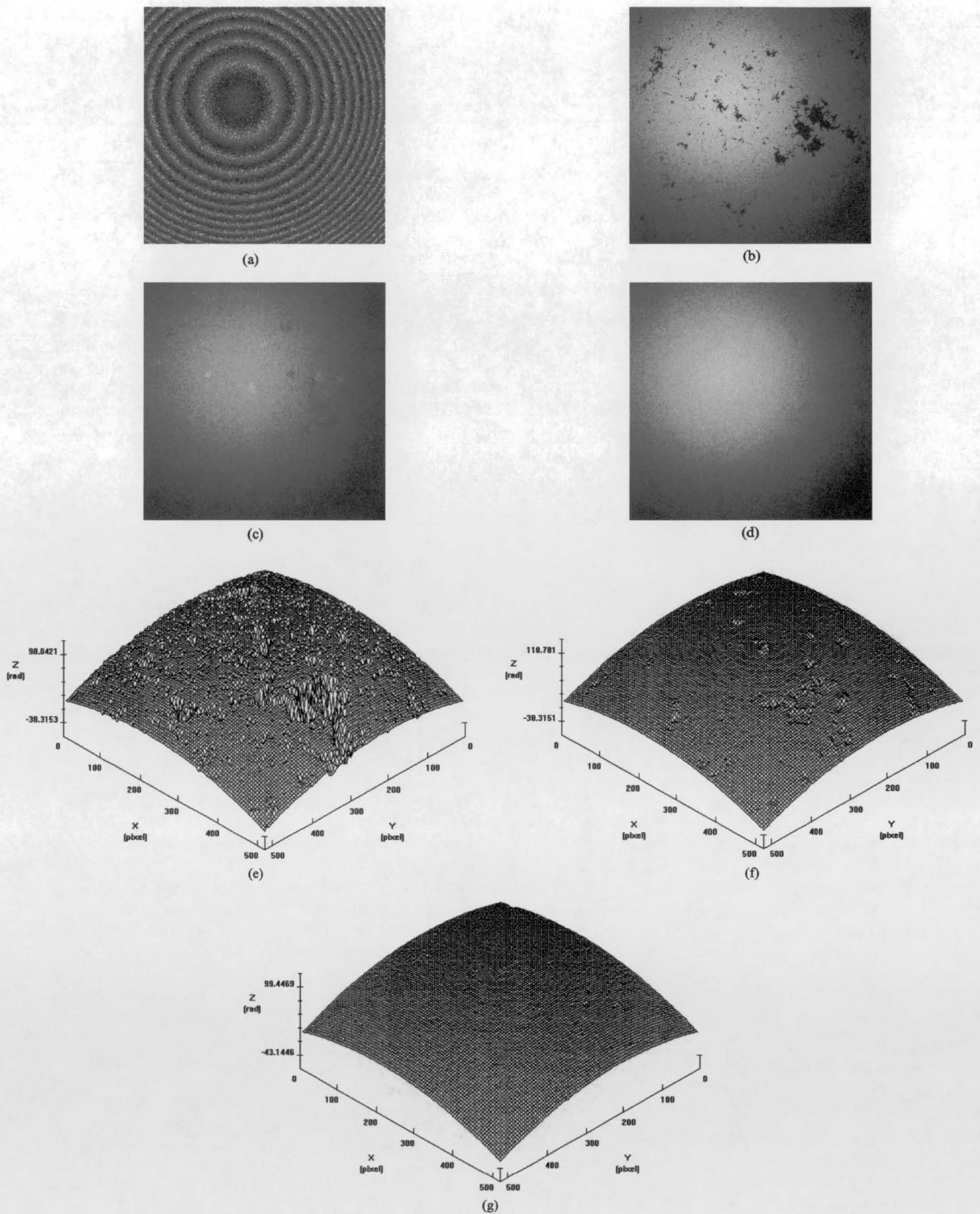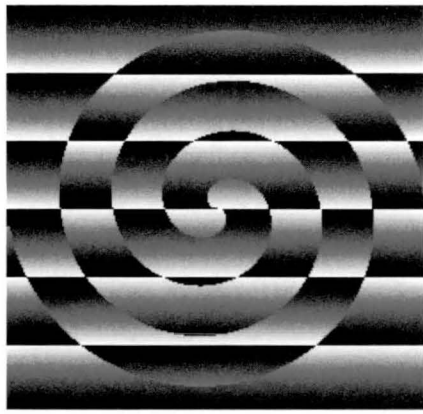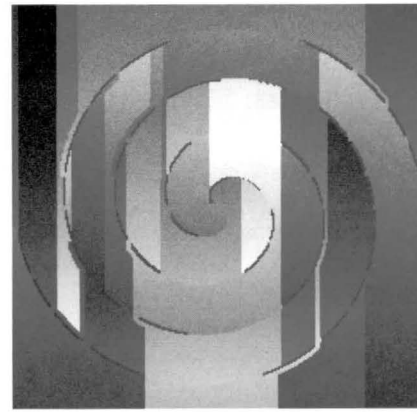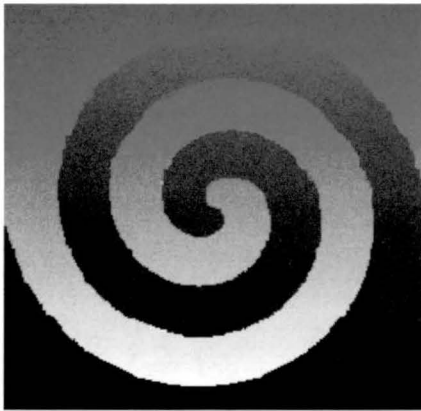
Fig. 3 Unwrapping of a simulated wrapped phase image with random noise: (a) wrapped phase image, (b) result unwrapped using the mask cut algorithm with the phase derivative variance map, (c) result unwrapped using the proposed algorithm with the phase derivative variance map, (d) result unwrapped using the proposed algorithm with the new quality map, (e) 3-D rendering of (b), (f) 3-D rendering of (c), and (g) 3-D rendering of (d).
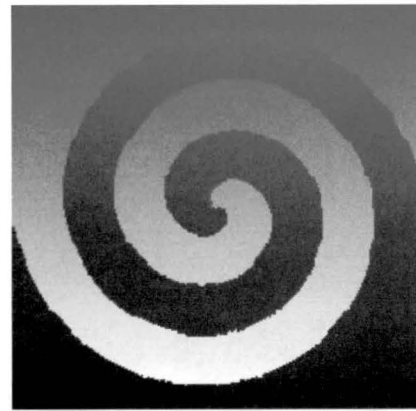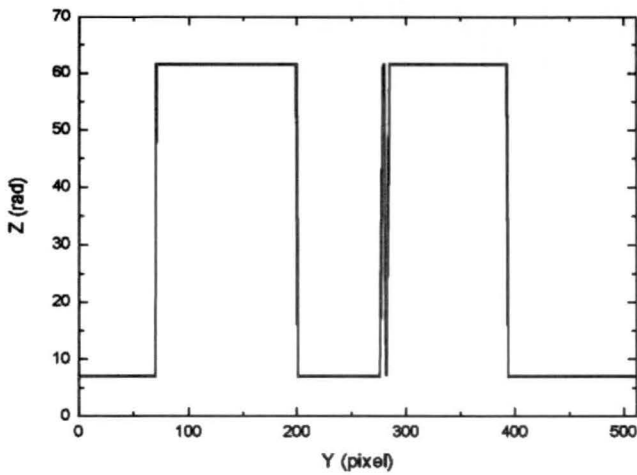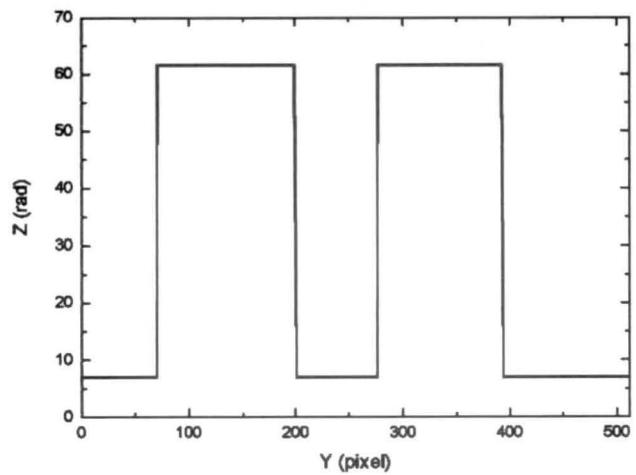
(a)

(b)

(c)

(d)

(e)

(f)

Fig. 4 Unwrapping of a simulated wrapped phase image with surface discontinuities: (a) wrapped phase image, (b) result unwrapped using the mask cut algorithm with the phase derivative variance map, (c) result unwrapped using the proposed algorithm with the phase derivative variance map, (d) result unwrapped using the proposed algorithm with the new quality map, (e) 2-D profile plot of (c) when $x=412$ pixels, and (f) 2-D profile plot of (d) when $x=412$ pixels.

quality map of Fig. 5(a) is shown in Fig. 5(b). As we can see, the wrapped phase map is corrupted by salt-and-pepper noise, especially in the area of the fiber undercut. In addition, in this area the dense fringe may cause undersampling problem.

Figure 5(c) shows the unwrapped phase map by use of the mask cut algorithm with the phase derivative variance map. The corresponding 3-D plot of Fig. 5(c) is shown in Fig. 5(d). We can see that in the noisy and rapidly changing part of the endface of the fiber connector, where the fiber
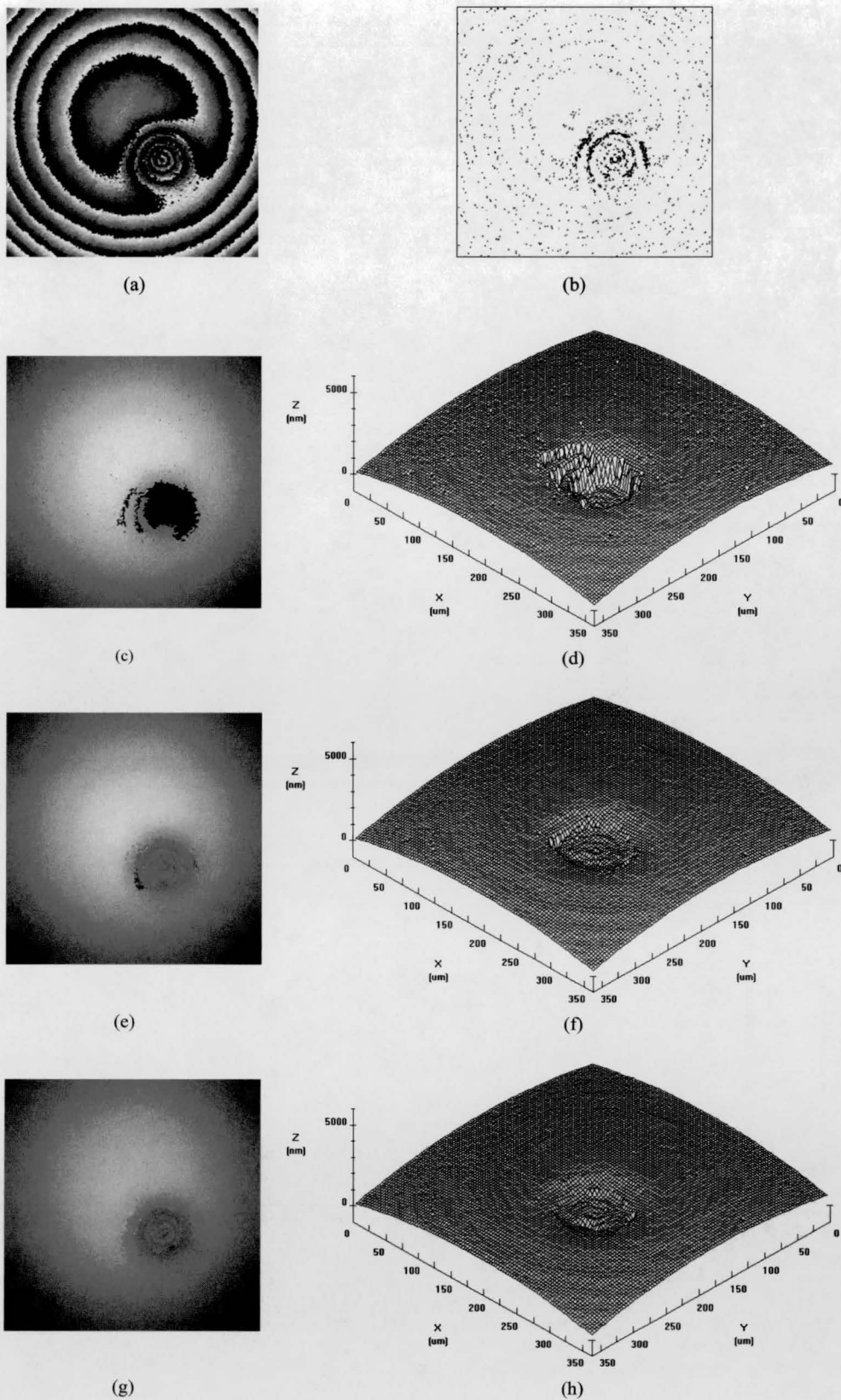
Fig. 5 Unwrapping of a wrapped phase image obtained from the measurement of an optical fiber connector endface: (a) wrapped phase image, (b) the new quality map of (a), (c) result unwrapped using the mask cut algorithm with the phase derivative variance map, (d) 3-D rendering of (c), (e) result unwrapped using the proposed algorithm with the phase derivative variance map, (f) 3-D rendering of (e), (g) result unwrapped using the proposed algorithm with the new quality map, and (h) 3-D rendering of (g).

ndface lies, the mask cut algorithm cannot generate a correct result. Figures 5(e) and 5(g) show the results unwrapped using the proposed algorithm with the phase derivative variance map and the new quality map, respectively. Figures 5(f) and 5(h) are their respective 3-D profiles. As shown in Figs. 5(e) and 5(f), the proposed algorithm can produce an almost correct result, although there is a trivial error that originates from the drawbacks of the phase derivative variance map. Apparently, when the new quality map is used as the original quality map to guide the placement of the branch cuts, the proposed algorithm copes well with the intractable wrapped data, producing an unwrapped result that is consistent and correct.

The execution time of the proposed algorithm varies from image to image and depends on the selection of the original quality map. The proposed algorithm was executed on a PC system, which contains a Pentium III processor that runs at a 800-MHz clock speed. The memory on this PC is 128 Mbyte RAM. When the new quality map is used as the original quality map and the tested images are 512 $\times$512 pixels in size, the execution time is about 3 s.

5 Conclusions

A fast, reliable quality-guided phase-unwrapping algorithm based on the placement of the branch cuts was proposed and tested. Because the phase-unwrapping path does not encircle any unbalanced residue and is always along the way from a higher reliability area to an area with low reliability, even in the worst case, the phase unwrapping error, if any, is limited to local minimum regions. Using the proposed new quality map as the original quality map to guide the placement of the branch cuts, the algorithm correctly produces consistent and reliable results even when noisy data, surface discontinuities, or undersampling are present.

Acknowledgments

References

1. V. V. Volkov and Y. Zhu, "Deterministic phase unwrapping in the presence of noise," *Opt. Lett.* **28**(22), 2156–2158 (2003).
2. W.-S. Li and X.-Y. Su, "Phase unwrapping algorithm based on phase fitting reliability in structured light projection," *Opt. Eng.* **41**(6), 1365–1372 (2002).
3. A. Baldi, "Two-dimensional phase unwrapping by quad-tree decomposition," *Appl. Opt.* **40**(8), 1187–1194 (2001).
4. M. A. Herraez, D. R. Burton, M. J. Lalor, and M. A. Gdeisat, "Fast two-dimensional phase-unwrapping algorithm based on sorting by reliability following a noncontinuous path," *Appl. Opt.* **41**(35), 7437–7444 (2002).
5. R. M. Goldstein, H. A. Zebker, and C. L. Werner, "Satellite radar interferometry: two-dimensional phase unwrapping," *Radio Sci.* **23**(4), 713–720 (1988).
6. J. M. Huntley, "Noise-immune phase unwrapping algorithm," *Appl. Opt.* **28**(15), 3268–3270 (1989).
7. R. Cusack, J. M. Huntley, and H. T. Goldrein, "Improved noise-immune phase-unwrapping algorithm," *Appl. Opt.* **34**(5), 781–789 (1995).
8. J. R. Buckland, J. M. Huntley, and S. R. E. Turner, "Unwrapping noisy phase maps by use of a mimimum cost matching algorithm," *Appl. Opt.* **34**(23), 5100–5108 (1995).
9. D. J. Bone, "Fourier fringe analysis: the two-dimensional phase unwrapping problem," *Appl. Opt.* **30**(25), 3627–3632 (1991).
10. Y. Xu and C. Ai, "Simple and effective phase unwrapping technique," *Proc. SPIE* **2003**, 254–263 (1993).
11. J. A. Quiroga, A. González-Cano, and E. Bernabeu, "Phase-unwrapping algorithm based on an adaptive criterion," *Appl. Opt.* **34**(14), 2560–2563 (1995).
12. W. Xu and I. Cumming, "A region growing algorithm for InSAR phase unwrapping," in *Proc. 1996 Int. Geoscience and Remote Sensing Symp.*, Lincoln, NE, pp. 2044–2046, IEEE, Piscataway, NJ (1996).
13. X. Su and W. Chen, "Reliability-guided phase unwrapping algorithm: a review," *Opt. Lasers Eng.* **42**(3), 245–261 (2004).
14. T. J. Flynn, "Consistent 2-D phase unwrapping guided by a quality map," in *Proc. 1996 Int. Geoscience and Remote Sensing Symp.*, Lincoln, NE, pp. 2057–2059, IEEE, Piscataway, NJ (1996).
15. D. C. Ghiglia and M. Pritt, *Two-Dimensional Phase Unwrapping: Theory, Algorithms, and Software*, Wiley, New York (1998).
16. X. Su, G. von Bally, and D. Vukicevic, "Phase-stepping grating profilometry: utilization of intensity modulation analysis in complex object evaluation," *Opt. Commun.* **98**(1–3), 141–150 (1993).

Yuangang Lu received his BE degree in mechanical engineering from Anhui University of Technology, China, in 1998 and his ME degree in mechanical engineering from Nanjing University of Aeronautics and Astronautics, China, in 2002. He is currently pursuing his PhD degree at the Shanghai Institute of Optics and Fine Mechanics, Academia Sinica, China. His research interests include optical interferometry and fringe analysis techniques.

Xiangzho Wang received his BE degree in electrical engineering from Dalian University of Science and Technology, China, in 1982 and his ME and DrEng degrees in electrical engineering from Niigata University, Japan, in 1992 and 1995, respectively. He is a professor of optical engineering with the Shanghai Insitute of Optics and Fine Mechanics, Academia Sinica, China. His research interests include optical metrology and optical information processing.

Guotian He: Biography and photograph not available.